

Exceptionally Slow Rise in Differential Reflectivity Spectra of Excitons in GaN: Effect of Excitation-induced Dephasing

Y. D. Jho* and D. S. Kim

Department of Physics, Seoul National University, Seoul 151-747, Korea

A. J. Fischer and J. J. Song

*Department of Physics and Center for Laser Research,
Oklahoma State University, Stillwater, Oklahoma 74078*

J. Kenrow,[†] K. El Sayed, and C. J. Stanton

Department of Physics, University of Florida, Gainesville, Florida 32611

Abstract

Femtosecond pump-probe (PP) differential reflectivity spectroscopy (DRS) and four-wave mixing (FWM) experiments were performed simultaneously to study the initial temporal dynamics of the exciton line-shapes in GaN epilayers. Beats between the A-B excitons were found *only for positive time delay* in both PP and FWM experiments. The rise time at negative time delay for the differential reflection spectra was much slower than the FWM signal or PP differential transmission spectroscopy (DTS) at the exciton resonance. A numerical solution of a six band semiconductor Bloch equation model including nonlinearities at the Hartree-Fock level shows that this slow rise in the DRS results from excitation induced dephasing (EID), that is, the strong density dependence of the dephasing time which changes with the laser excitation energy.

PACS numbers: 78.47.+p, 42.65.-k, 78.20.-e

*Current Address: National High Magnetic Field Laboratory, Florida State University, Tallahassee, FL 32310; Electronic address: ydjho@magnet.fsu.edu

[†]Current Address: Dept. of Electrical and Computer Engineering, University of the Pacific, Stockton, CA 95211

I. INTRODUCTION

Group III nitride semiconductors such as GaN and InGaN have become important materials owing to their optoelectronic device applications in the blue and ultraviolet spectral range and their use in high temperature electronic devices. The demonstration of InGaN multiple quantum well laser diodes[1] has also inspired tremendous research interest in the nitride-based materials. Transient four-wave mixing (FWM) studies on GaN were performed to investigate the intrinsic excitonic properties[2, 3] and the influence of electron spins on exciton-exciton interaction[4]. Femtosecond pump-probe (P-P) measurements were done by C.-K. Sun *et al.* on InGaN[5] and n-doped GaN[6] to investigate the fast carrier cooling. Time-resolved studies of coherent acoustic phonons in GaN and GaN/InGaN systems [7, 8, 9, 10], as well as coherent optical phonons[11] were performed. Recently, field dependent carrier decay dynamics were done by Jho *et al.*[12, 13]

In the FWM experiments on GaN, quantum beats of excitons and their phase changes via polarization configurations have been studied and exciton-phonon interaction rates were deduced. Nevertheless, there are still not a lot of time-domain studies regarding the coherent response of excitons in GaN including many body effects.

The FWM line shapes not only discriminate between homogeneous broadened and inhomogeneous broadened systems[2] but also provide information on the carrier-carrier interaction[14]. For instance, time-integrated (TI) FWM signals at negative time delays have been observed in GaAs quantum wells[15, 16] and understood by local-field effects[15, 16] or excitation-induced depasing (EID)[17] which are incorporated into the semiconductor Bloch equations. In addition, it was argued that EID dominates at a moderately low exciton density ($< 10^{16}cm^{-3}$) and gives a strong contribution to TI-FWM in the co-linearly polarized geometry.[17]

In this work we report the comparative studies of femtosecond degenerate pump-probe (PP) differential reflectivity spectroscopy (DRS) measurements and time-integrated (TI)-FWM experiments on GaN epilayers as a function of excitation energy at low carrier excitation density. In addition, we have also performed PP differential transmission spectroscopy on a thin GaN sample, though not simultaneously with FWM. Our results show that the quantum beats as revealed in previous studies[2, 3, 4] are the same both in PP and FWM and exist *only for positive time delay*. Results further show that the DRS and FWM differ at

negative time delays, with the DRS signal persisting longer at the negative delays in spite of inhomogenous broadening. Calculations based on a six-band semiconductor Bloch equation model solved in the Hartree-Fock level show that this difference arises from EID, that is, the dephasing time depends on the carrier density excited by the laser pulse.

II. EXPERIMENTAL SCHEME

The GaN samples used in this work were a 7.2 μm -thick and a 2 μm -thick epilayer grown with the wurtzite structure on a (0001) sapphire substrates by metalorganic chemical vapor deposition. The second harmonic of a femtosecond Ti-sapphire laser in the high-energy region of the tuning (705 nm - 710 nm) was used, with 150-fs pulse-width. As shown in the Fig. 1(a), we have performed both FWM and differential reflectivity spectroscopy (DRS) *simultaneously* in the reflection geometry on 7.2 μm -thick sample. To compare the differential reflection spectra with the differential transmission spectra (DTS), a 2 μm -thick sample was also used. The pump and probe pulses were at the same wavelengths and collinear polarization. All measurements were performed at 11 K unless otherwise noted (c.f. Fig. 7). To reduce the effect of the laser noise, we used a differential amplification scheme after dividing the probe beam (\mathbf{k}_1) into two. With this scheme, the DRS signal can be as small as 10^{-4} .

In Fig.1(b), the spectrally resolved (SR) FWM data (solid line) at 11 K is shown together with the spectrum of laser for detunings of 0 meV (dashed) and 20 meV (dotted) from the center of the exciton peaks. There is no time delay between pump and probe. The two peaks of Fig. 1 (b) correspond to the $\Gamma_9^V - \Gamma_7^C$ exciton (A exciton transition) and the $\Gamma_7^V - \Gamma_7^C$ exciton (B exciton transition), which are caused by crystal field and spin-orbit coupling. The dashed and dotted lines are the spectrum of laser at the center of the exciton resonances and at 20 meV above the resonance. The linewidth of peaks are measured to be 2.1 meV for the A exciton, and 2.5 meV for the B exciton. The energy difference of the two excitons is about 8 meV.

The power of the pump (probe) pulse which is in the reflection direction of \mathbf{k}_1 (\mathbf{k}_2) was 0.5 mW (0.1 mW). The two beams are focused onto a 100 μm spot with the external-crossing angle of 6° . From the measured absorption coefficient, we estimate the initial carrier density to be $5 \times 10^{15} \text{cm}^{-3}$ at the center of the exciton resonances (3.497 eV)[18]. There was no

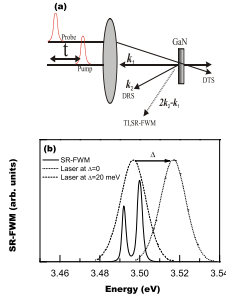


FIG. 1: (a) Experimental schematic showing the simultaneous measurement of the four-wave mixing (FWM) and pump-probe (PP) differential reflectivity spectra (DRS). In the reflection geometry, the wave vector of the pump (\mathbf{k}_1) and probe (\mathbf{k}_2) are shown. (b) The spectrally resolved (SR)-FWM data at 11 K (solid line) for $t=0$ (i.e. no time delay between pump and probe). The line-width of the peaks are 2.1 meV (A exciton) and 2.5 meV (B exciton). The dashed and dotted line show the laser spectrum with detuning $\Delta = 0$ (and the center between the two excitons) and 20 meV respectively.

detectable change of decay time in the FWM for carrier densities ranging from 10^{15}cm^{-3} to $5 \times 10^{16} \text{cm}^{-3}$.

III. RESULTS AND DISCUSSION

Fig. 2 shows the simultaneous measurements of the DRS and FWM at the excitation energy of (a) 3.497 eV, (b) 3.507 eV, and (c) 3.517 eV. The FWM data were scaled with the DRS data for comparison. In both the PP and FWM data, the strongest signal was observed at the exciton resonance, 3.497 eV. This is in the middle of the A and B excitons. Here Δ , the detuning is chosen to be the energy above 3.497 eV and hence the figures correspond to detunings of $\Delta = 0, 10$ and 20 meV respectively. The PP data and the FWM, in positive time delay, show similar features, namely that of beating between the A and B excitons. This beating is strongest for $\Delta = 0$, i.e. at the resonance and has a period of about 500 fs. This period is consistent with the SR-FWM that showed the energy difference of 8 meV between A and B excitons (c.f. Fig. 1).

One puzzling difference between the PP DRS and FWM signals is the behavior at negative time delay. The PP signals in negative time delay persist much longer than the FWM and do

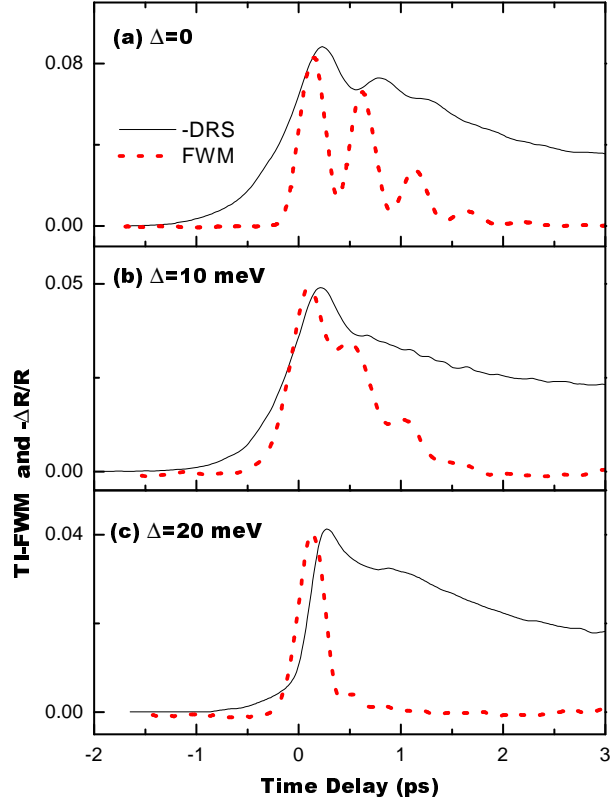


FIG. 2: Experimental DRS (solid lines) and FWM (dotted lines) at different detunings Δ above the exciton resonance energy ($= 3.497$ eV). The FWM and DRS both show oscillations at positive time delay associated with beating between the A and B excitons. At negative time delay, the DRS shows a slow rise time while the rise time of the FWM is determined by the pump pulse. Exciton beating is not observed in negative time delay.

not show the A-B exciton beatings. The DRS behavior is strongest at the exciton resonance ($\Delta = 0$), but becomes less pronounced as one increases the detuning ($\Delta = 20$ meV) and excites further into the band. The values of the DRS rise times obtained from first order exponential fits were 445 fs ($\Delta = 0$), 381 fs ($\Delta = 10$ meV), and 183 fs ($\Delta = 20$ meV). The error in determining the rise time is less than 20 fs for all measurements. The rise times of FWM were less than 200 fs for all excitation energies and comparable to the pump laser duration.

The fact that there is a fast rise time in negative delay in the FWM is not surprising. To

see a slow rise in the FWM signal in the negative time delay requires that the sample be very clean and that inhomogeneous broadening is weak.[15, 16] Inhomogeneous broadening will wash out any negative time signal in the FWM.

In Fig. 3 we compare the rise times of the DRS versus the FWM signal. Since the values of FWM decay time (τ_{FWM}) for positive delay and zero detuning ($\Delta = 0$) in Fig. 3 are at least three times larger than the FWM rise times, this indicates that the spectra are inhomogeneously broadened in these samples.[2, 15] In fact, the rise time of the FWM signal appears to be limited by the pulse duration, again consistent with strong inhomogeneous broadening. As a result, one would not expect to see a FWM signal in the negative time delay since it has been shown that this would occur only in a homogeneously broadened system.[15, 16]

In contrast, the differential pump-probe reflectivity spectra can have a signal at negative delay, even with inhomogeneous broadening. This is related to the free polarization decay (FPD) of the *probe* pulse which plays a role in the DRS signal at negative time delays. Note however, that the FPD of the probe pulse does not effect the FWM. This is because while the FPD of the probe pulse will produce a signal in the probe direction (\mathbf{k}_2), it does not produce a signal in the FWM direction $2\mathbf{k}_2 - \mathbf{k}_1$.[16]

The FPD persists when the probe precedes the pump even in an inhomogeneously broadened system. This leads to a rise time with an effective time constant T_2^* . T_2^* is given approximately by the inverse of frequency spread due to inhomogeneous broadening $1/\Delta\omega$ and is shorter than T_2 , the homogeneous dephasing time.[19] If the pump pulse (which is now after the probe pulse for negative time delay) overlaps with the tail of the FPD of the probe pulse, then it may be possible to produce a signal in the probe pulse.

It has been shown in DTS, that the overlap of the pump with the tail of the probe polarization generates a transient diffraction grating with wavevector $\mathbf{k}_2 - \mathbf{k}_1$. This transient grating can lead to a diffraction of part of the pump pulse with wave vector \mathbf{k}_1 into the probe direction $\mathbf{k}_1 + (\mathbf{k}_2 - \mathbf{k}_1)$. This is the qualitative origin of the well-known coherent oscillations in semiconductors[20] or the perturbed free polarization decay term[19]. The spectral oscillations induced from the transient grating have no correlation with the exciton oscillations seen in Fig. 2(a) at positive time delay. These coherent oscillations are readily observed in our sample, and are shown in Fig. 4 for the spectrally resolved DRS signal. The spectral oscillations, depend on the time delay as well as the detuning from the exciton

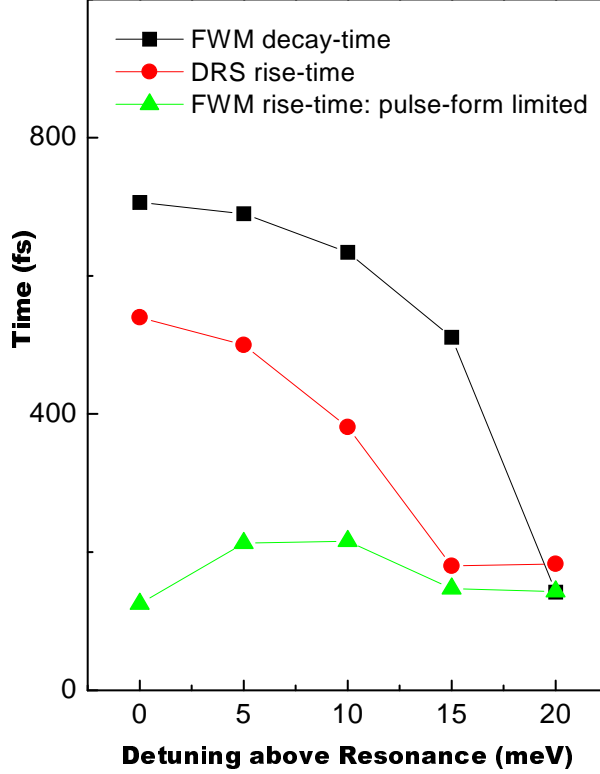


FIG. 3: The rise and decay times of the DRS and FWM as a function of laser detuning above the exciton resonance. The DRS rise time is given by the circles, the FWM rise time by the triangles, and FWM decay time by the squares. Note that the decay time of the FWM and the rise time of the DRS are comparable while the rise time of the FWM appears to be determined by the pump laser pulse width.

resonance.

However, a solution of the density matrix equation[19] without incorporating the exciton-exciton interaction or EID, shows that, when integrated over frequency, *the different spectral oscillatory signals cancel out and the net result is that DTS spectra at each negative time delay is integrated out to be zero*. This result should also hold for the DRS spectrum when the excitation is deep within the band continuum. In fact, Fig. 2(c) precisely shows this effect. (In addition, for large detuning and excitation within the band, the dephasing time T_2 should be much shorter than for excitations between the A and B excitons).

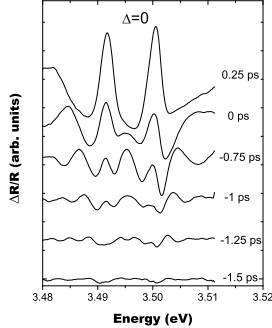


FIG. 4: Experimentally measured spectral resolved DRS. The pump detuning is $\Delta = 0$, i.e. between the A and B exciton resonances. The time delay between pump and probe is given for each trace in the figure.

Below the continuum band edge, the situation is more complex. To study this effect more thoroughly, calculations were performed based on the Semiconductor Bloch Equations.

IV. CALCULATIONS

To better understand the origin of the slow rise-time of the DRS signal in Fig. 2, we have calculated both the differential reflection (DRS) and differential transmission spectra (DTS) by solving a coupled six-band semiconductor Bloch equation model[22, 23] including all Hartree-Fock nonlinearities. From the semiconductor Bloch equations, the dielectric response is calculated. Typically, the reflection is much more sensitive to the real part of the dielectric response while the transmission is more sensitive to the imaginary part of the dielectric response. In our calculations, we have included carrier scattering on a phenomenological level to allow for the relaxation of the photo-excited carriers back to equilibrium. In addition, we have included excitation induced dephasing (EID)[17, 24] to allow for the change in the carrier dephasing time as the density of excited carriers changes with the pump laser pulse.

In the framework of EID, the inverse polarization decay time is given by

$$1/T_2 = 1/T_{2,0} + n/T_{2,1}, \quad (1)$$

and is a linear function of the induced carrier density, n . $T_{2,1}$ corresponds to the carrier-carrier scattering time as the carriers are photoexcited in a nonthermalized distribution. At

low carrier densities, scattering such as electron-electron is a linear function of the density. At higher densities, screening effects can become important and change the density dependence. Note that the polarization decay time has the important property that it is long when the probe precedes the pump since no carriers have been created yet and the decay time becomes shorter when the probe comes after the pump pulse which creates photoexcited carriers.

We chose the low density dephasing time, $T_{2,0}$ to be 1 ps. By numerically integrating the semiconductor Bloch equations, we computed the induced polarization with and without the pump pulse present. The corresponding dielectric response, which determines the reflection and transmission spectra, is obtained from the Fourier transform of the probe polarization.

In calculating the dielectric response, we do not allow for *intraband* changes to the dielectric function. This should be less important when one excites below the band edge since there are no free carriers available to screen out the laser pulse and give a Drude-like contribution to the dielectric function, which can be important in the reflectivity. However, this becomes more important when a large number of free carriers are excited above the band gap and for strong excitation above the gap, may even dominate the signal.[25, 26] In addition, we do not include diffusion of carriers away from the surface[25, 26, 27] of the sample in our calculations. The intent of the calculations is to understand the *initial* behavior of the PPRS and DTS spectra. Diffusion effects become important on a time scale longer than 1 ps and should be included along with more accurate scattering models in more detailed studies for longer times.

Results of the numerical solution to the model are shown in figure 5. Figure 5 shows the computed DTS and DRS signals as a function of delay between the pump and probe pulses. Fig. 5 (a) gives the result when the pump and probe are both at resonance with the excitons (excitation between the A and B excitons) and EID as well as carrier scattering are included (i.e. both terms in eq. 1). The corresponding results when EID was excluded (i.e., only the first term on the left hand side of eq. 1 is included) are shown in Fig. 5(b). Note that both figures show the oscillations resulting from A and B exciton beating in both the DRS and DTS signals at positive time delay.

Our simulation also reproduces the slow rise-time of the DRS signal in Fig. 2(a) *only if EID is included* (cf. Fig. 5(a)). However, if EID is excluded, the effect vanishes and the signal strength is diminished by 60 % (cf. Fig. 5(b).) In this case, oscillations occur at negative time in the in the DRS. It is important to note that this behavior is *not seen*

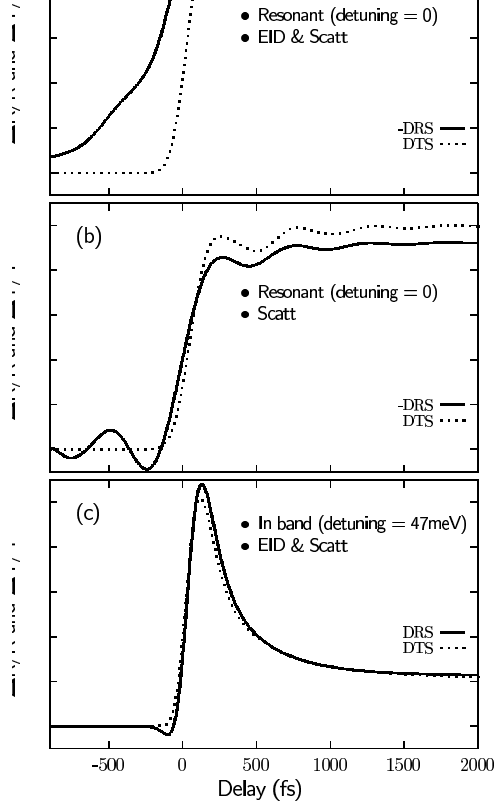


FIG. 5: The calculated differential reflection (DRS) and differential transmission spectra (DTS) as a function of delay time between the pump and probe pulses based on the Semiconductor Bloch Equations. In (a), the laser excitation energy is resonant between the excitons. Scattering as well as excitation induced dephasing (EID) is included in the simulation (both terms in eq. 1.). As can be seen, the DRS signal has a slower rise time than the DTS signal. In (b), the laser excitation energy is resonant with the excitons but only the first scattering term in eq. 1 is included. Here both the DRS and DTS signal have similar rise times. In (c), the laser excitation energy is deep into the band. Both EID and scattering are included in simulation. The rise time of the DRS is faster than for laser excitation energy at the exciton (a).

for the corresponding DTS signal where the rise times are unaffected by EID. However, a comparison of the two DTS signal strengths shows that the inclusion of the EID enhances the signal strength by 40%. When probing the samples at laser energies deep into the band, (Fig. 5(c)) we find that the rise time of the DRS signal is now faster in agreement with experiment (cf. Fig. 2, 3), and shows little difference with the DTS signal. Of course, deep within the band, one must take into account the other effects previously mentioned.

In addition to calculating the PP DRS and DTS signals, we have also calculated the FWM signal. The calculations agree with the experimental results of Fig. 2 showing: (i) the decay of the FWM signal as one increases the detuning, Δ and excites further into the band, (ii) that the EID does not change the rise-times of the FWM at the exciton energy or in the band, and (iii) that the oscillations in the FWM for positive time delay are out of phase with the oscillations in the DRS. Similar results were also seen in calculations of the FWM in high-quality GaAs quantum wells.[24]

To investigate further our theoretical prediction that the DRS signal shows a slow rise time while the DTS signal shows a fast rise time, further experimental pump-probe measurements were performed in both the reflection and transmission geometry on bulk GaN. To be able to perform transmission measurements, the $2\ \mu\text{m}$ thick samples were used. The results are shown in Fig. 6. The excitation spectrum was chosen to excite both the A and B exciton simultaneously. The temporal traces of the DRS and DTS show the qualitative behavior similar to our theoretical calculations including EID; a much slower rise time in the DRS as opposed to the more rapid, pulse-form limited rise of the DTS. Note that there is a negative dip in DTS near zero delay. This can possibly be caused by distortion of the pulse.[28] We note that the thickness of $2\ \mu\text{m}$ is much larger than the penetration depth of GaN, hence, any excitonic signals must have been absorbed and the DTS signal is an order of magnitude larger than DRS signal due to relatively small transmission compared to the pump induced transmission change.

One possible reason for the differences in the early time behavior of the DTS versus the DRS signals is that they measure different quantities. The DTS signal is related to the imaginary part of the dielectric function which is a local function of frequency depending on the central frequency of the probe pulse. The DRS depends more strongly on the real part of the dielectric function. Hence, through the Kramers-Kronig transformation, the DRS is sensitive to spectral regions above and below the central probe frequency.

In Fig. 7 we investigate the temperature dependence of the DRS and FWM for $\Delta = 0$. The polarization decay time is given by the eq. 1. The first term on the right represents decay due to scattering with impurities or phonons which is not strongly density dependent and the second term represents the density dependent scattering mechanisms such as carrier-carrier (electron-electron, electron-hole etc). We expect the first term to be much more temperature dependent since, for example, electron-phonon scattering depends on the phonon occupation

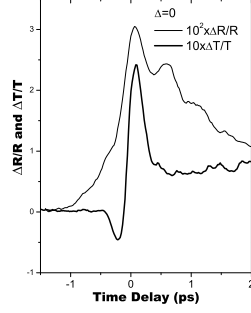


FIG. 6: Experimental DRS (solid line) and DTS (dotted line) for a 2 μm -thick GaN sample. The DRS and DTS signals were multiplied by the values in the figure for comparison purposes and the frequency of the pump was chosen to be between the A and B excitons ($\Delta = 0$). The DRS shows a slow rise time for negative delays while the DTS does not show a slow rise time similar to the calculations in Fig. 5(a).

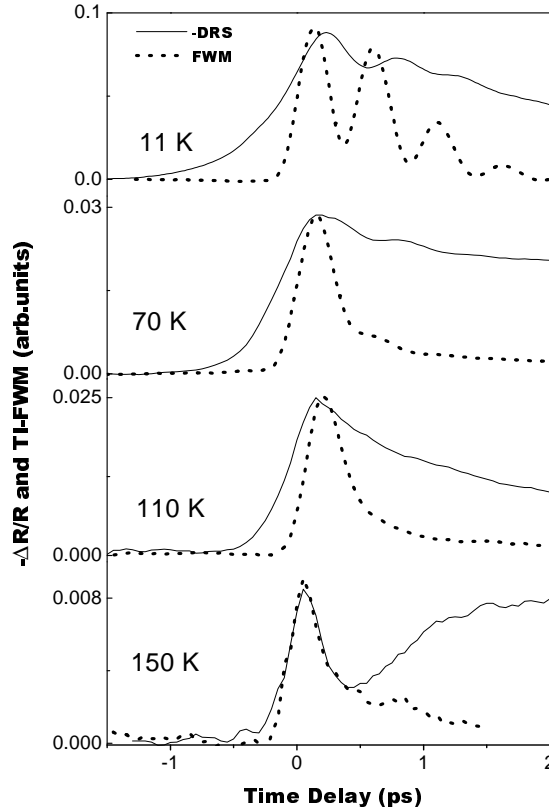


FIG. 7: Temperature dependence of the FWM (dotted line) and DRS (solid line) signals near the exciton resonance at 10, 70, 110, and 150 K for a 7.2 μm -thick GaN epilayer. The detuning $\Delta = 0$.

number which depends strongly on temperature. Carrier-carrier scattering is only weakly temperature dependent. Fig. 7 shows the data of the DRS (solid lines) and TI-FWM (dotted lines) measured at four different temperatures ($T=11, 70, 110,$ and 150 K). The laser was tuned to excite both the A exciton and B exciton. We note that as the temperature is increased, the rise time at negative delay of the DRS becomes more rapid and approaches that of the FWM. We see that near 150 K, both the DRS and FWM have nearly the same rise time. In addition, the DRS rise time and FWM decay time (for positive delay) show a similar tendency to decrease with increasing temperature. The rapid decrease of FWM decay time starting from around 150 K is due to the dominance of optical phonons as a scattering mechanism for dephasing of excitons.[2] Note that the rapid phonon scattering time above 150 K also has the effect of rapidly damping out the FPD and hence the DRS signal now has a fast rise time.

Our theoretical results based on EID are suitable only for the low density regime where the nonlinear response near the band edge is dominated by excitonic screening of the carrier-carrier Coulomb potential.[17] As we increase the carrier density ten-fold as shown in Fig. 8, EID is not dominant any more and the slow rise signal which was observed in Fig. 2 is superimposed by a faster rise with opposite sign. The sign change in Fig. 8 could possibly be associated with the band-gap renormalization and reduction of the Coulomb enhancement factor which occurs for high density photoexcitation.[5, 21]

V. CONCLUSION

In this work, we have studied the initial temporal dynamics in GaN epilayers through the simultaneous measurement of PP DRS and FWM. For resonant excitation of the A and B excitons, we have observed an unusually slow rise time in *negative time delay* only in the PP DRS in contrast to the FWM and DTS signals which show a more rapid rise time. These differences can be explained by excitation induced dephasing and the fact that the FPD of the probe pulse can contribute to the PP signal, but not the FWM. We have shown from simulations of the Semiconductor Bloch Equations, that EID strongly alters the line-shape for the DRS signal. With no scattering or excitation induced dephasing, the negative time delay in the DRS shows oscillations. With scattering and EID, we obtain a slow rise time at the exciton resonance for the DRS but not for the FWM or DTS signal. For energies above

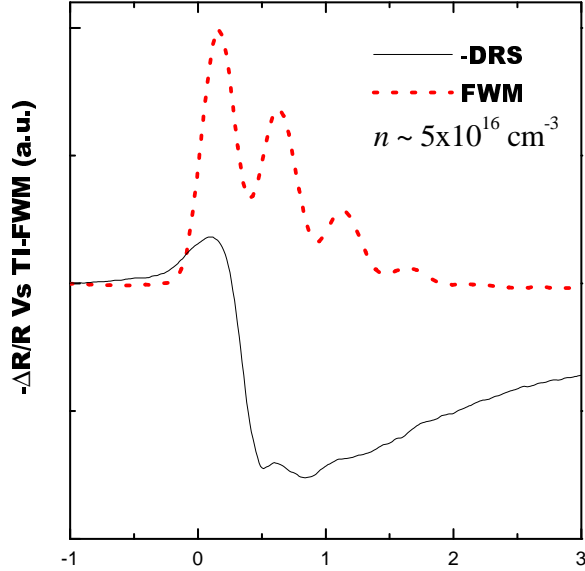


FIG. 8: The DRS (solid line) and FWM (dotted line) in a 7.2 μm -thick GaN epilayer, for high carrier density photoexcitation ($\sim 5 \times 10^{16} \text{cm}^{-3}$).

the band edge or at higher temperature where scattering is much stronger, the DRS signal has a short rise time and the FWM signal decays rapidly even at positive delay times.

Acknowledgments

This work was supported by MOST (the National Research Laboratory Program) and KOSEF (the Center for Strongly Correlated Materials Research, and Grant No. 97-0702-03-01-3). The work at U. of Florida was supported in part through Department of Energy through grant DE-FG05-91-ER45462 and the National Science Foundation through grant DMR-9817828.

-
- [1] S. Nakamura, S. Pearton, and G. Fasol, *The Blue Laser Diode, the Complete Story*, Springer, Berlin (2000).
- [2] A. J. Fischer, W. Shan, G. H. Park, J. J. Song, D. S. Kim, D. S. Yee, R. Horning, and B. Goldenberg, *Phys. Rev. B*, **56**, 1077 (1997).

- [3] S. Pau, J. Kuhl, F. Scholz, V. Haerle, M. A. Khan, and C. J. Sun, *Phys. Rev. B* **56**, R12718 (1997) ; R. Zimmermann, A. Euteneuer, J. Mobius, D. Weber, M. R. Hofmann, W. W. Ruhle, E. O. Gobel, B. K. Meyer, H. Amano, and I. Akasaki, *ibid.* **56**, R12722 (1997).
- [4] T. Aoki, G. Mohs, M. Gonokami, and A. A. Yamaguchi, *Phys. Rev. Lett.* **82**, 3108 (1999).
- [5] C.-K. Sun, F. Vallee, S. Keller, J. E. Bowersand, P. DenBarrs, *Appl. Phys. Lett.* **70**, 2004 (1997).
- [6] C.-K. Sun, Y.-L. Huang, S. Keller, U. K. Mishra, and S. P. DenBaars, *Phys. Rev. B* **59**, 13 535 (1999).
- [7] J.S. Yahng, Y. D. Jho, K. J. Yee, E. Oh, J. C. Woo, D. S. Kim, G. D. Sanders, and C. J. Stanton, *Appl. Phys. Lett.* **80**, 4723 (2002).
- [8] C.-K. Sun, J.-C. Liang, C. J. Stanton, A. Abare, L. Coldren, S. P. DenBaars, *Appl. Phys. Lett.* **75**, 1249 (1999).
- [9] C. J. Stanton, G. D. Sanders, R. Liu, C. S. Kim, Y. S. Yahng, E. Oh, D. S. Kim, and C.-K. Sun, in "Ultrafast Phenomena in Semiconductors VI", F. Tsen editor, *Proceedings of SPIE* Vol. 4643, 124 (2002).
- [10] C.-K. Sun, J. C. Liang, S. P. DenBaars, D. S. Kim, Y. D. Cho, G. D. Sanders, J. Simmons, and C. J. Stanton, *Superlattices and Microstructures*, **27**, 593 (2000).
- [11] K. J. Yee, K. G. Lee, E. Oh, D. S. Kim, and Y. S. Lim, *Phys. Rev. Lett.* **88** 105501 (2002).
- [12] Y. D. Jho, J. S. Yhang, E. Oh, and D. S. Kim, *Appl. Phys. Lett.* **79** 1130 (2001).
- [13] Y. D. Jho, J. S. Yhang, E. Oh, and D. S. Kim, *Phys. Rev. B* **66** 035334 (2002).
- [14] J. Shah, in *Ultrafast Spectroscopy of Semiconductors and Semiconductor Nanostructures*, Springer Ser. Solid-State Sci., Vol. 115 (Springer, Berlin, Heidelberg 1996), and references therein.
- [15] M. Wegener, D. S. Chemla, S. Schmitt-Rink, and W. Schafer, *Phys. Rev. A* **42**, 5675 (1990).
- [16] K. Leo, M. Wegener, J. Shah, D. S. Chemla, E. O. Gobel, T. C. Damen, S. Schmitt-Rink, and W. Schafer, *Phys. Rev. Lett.* **65**, 1340 (1990).
- [17] H. Wang, K. B. Ferrio, D. G. Steel, Y. Z. Hu, R. Binder, and S. W. Koch, *Phys. Rev. Lett.* **71**, 1261 (1993); Y. Z. Hu, R. Binder, and S. W. Koch, *Phys. Rev. B* **47**, 15 60 (1993).
- [18] A. J. Fischer, W. Shan, J. J. Song, Y. C. Chang, R. Horning, and B. Goldenberg, *Appl. Phys. Lett.* **71**, 1981 (1997).
- [19] C. H. Brito Cruz, J. P. Gordon, P. C. Becker, R. L. Fork, C. V. Shank, *IEEE J. Quantum*

- Electron. **24**, 261 (1988).
- [20] S. W. Koch, N. Peyghambarian, and M. Lindberg, J. Phys. C **21**, 5229 (1988).
- [21] P. Langot, R. Tommasi, and F. Vallee, Phys. Rev. B **54**, 1775 (1996); R. Tommasi, P. Langot, and F. Vallee, Appl. Phys. Lett. **66**, 1361 (1995).
- [22] J. A. Kenrow, K. El Sayed and C. J. Stanton, Phys. Rev. B **58**, R13399 (1998).
- [23] Y. Z. Hu, R. Binder, and S. W. Koch, Phys. Rev. B. **47**, 15679 (1993).
- [24] K. El Sayed, D. Birkedal, V. G. Lyssenko, and J. M. Hvam, Phys. Rev. B **55**, 2456 (1997); H. Wang, J. Shah, T. C. Damen, and L. N. Pfeiffer, Solid State Commun. **91**, 869 (1994); E. J. Mayer, G. O. Smith, V. Heuckeroth, J Kuhl, K. Bott, A. Schulze, T. Meier, D. Bennhardt, S. W. Koch, P. Thomas, R. Hay, and K. Ploog, Phys. Rev. B **50**, 14730 (1994).
- [25] S. Zollner, K. D. Myers, K. G. Jenson, J. M. Dolan, D. W. Bailey, and C. J. Stanton, Solid State Commun. **104**, 51 (1997)
- [26] S. Zollner, K. D. Myers, J. M. Dolan, D. W. Bailey, and C. J. Stanton, Thin Solid Films **313**, 568 (1998).
- [27] D. W. Bailey and C. J. Stanton, Appl. Phys. Lett. **60**, 880 (1992).
- [28] D. S. Kim, J. Shah, D. A. B. Miller, T. C. Damen, W. Schafer, and L. N. Pfeiffer, Phys. Rev. B **48**, 17902 (1993).